Mismatch repair *hMSH2*, *hMLH1*, *hMSH6* and *hPMS2* mRNA expression profiles in precancerous and cancerous urothelium

DIMITRA P. VAGELI[1], STAVROS GIANNOPOULOS[2], SOTIRIOS G. DOUKAS[1], CHRISTOS KALAITZIS[2], STILIANOS GIANNAKOPOULOS[2], ALEXANDRA GIATROMANOLAKI[3], GEORGE K. KOUKOULIS[1] and STAVROS TOULOUPIDIS[2]

[1]Department of Pathology, Medical School, University of Thessaly, Larissa, Thessaly 41110; Departments of [2]Urology and [3]Pathology, Medical School, Democritus University of Thrace and University Hospital of Alexandroupolis, Alexandroupolis 68100, Greece

Received July 4, 2012; Accepted September 26, 2012

DOI: 10.3892/ol.2012.979

Abstract. Changes in the expression of the mismatch repair (MMR) genes *hMSH2*, *hMLH1*, *hMSH6* and *hPMS2* reflect dysfunction of the DNA repair system that may allow the malignant transformation of tissue cells. The aim of the present study was to address the mRNA expression profiles of the mismatch DNA repair system in cancerous and precancerous urothelium. This is the first study to quantify MMR mRNA expression by applying quantitative real-time PCR (qPCR) and translate the results to mRNA phenotypic profiles (r, reduced; R, regular or elevated) in bladder tumors [24 urothelial cell carcinomas (UCCs) and 1 papillary urothelial neoplasm of low malignant potential (PUNLMP)] paired with their adjacent normal tissues (ANTs). Genetic instability analysis was applied at polymorphic sites distal or close to the *hMSH2* and *hMLH1* locus. Presenting our data, reduced *hMSH2*, *hMSH6* and *hPMS2* mRNA expression profiles were observed in cancerous and precancerous urothelia. Significantly, the ANTs of UCCs revealed the highest percentages of reduced *hMSH2* (r_2), *hMSH6* (r_6) and *hPMS2* (p_2) mRNA phenotypes relative to their tumors ($P<0.03$). In particular, combined r_2r_6 ($P<0.02$) presented a greater difference between ANTs of low-grade UCCs vs. their tumors compared with ANTs of high-grade UCCs ($P=0.000$). Reduced *hMLH1* (r_1) phenotype was not expressed in precancerous or cancerous urothelia. The *hMSH6* mRNA was the most changed in UCCs (47.8%), while *hMSH2*, *hMLH1* and *hPMS2* showed overexpression (47.8, 35 and 30%, respectively) that was associated with gender and histological tumor grading or staging. Genetic instability was rare in polymorphic regions distal to *hMLH1*. Our data reveal a previously unrecognized *hMSH2* and *hMSH6* mRNA combined phenotype (r_2r_6) correlated with a precancerous urothelium and show that *hMLH1* is transcriptionally activated in precancerous or cancerous urothelium. In the present study, it is demonstrated that reduction of *hMSH6* mRNA is a frequent event in bladder tumorigenesis and reflects a common mechanism of suppression with *hMSH2*, while alterations of *hMSH2* or *hMLH1* mRNA expression in UCCs does not correlate with the allelic imbalance of polymorphic regions harboring the genes.

Correspondence to: Dr Dimitra Vageli, Department of Pathology, Medical School, University of Thessaly, Viopolis, Larissa, Thessaly 41110, Greece
E-mail: vagelidim@yahoo.gr; vagelidim@med.uth.gr

Key words: bladder tumors, urothelial cell carcinoma, papillary urothelial neoplasm of low malignant potential, normal urothelium, *hMSH2*, *hMLH1*, *hPMS2*, *hMSH6*, quantitative real-time PCR

Introduction

The most common histological type of bladder cancer is urothelial cell carcinoma (UCC) or transitional cell carcinoma (TCC). Papillary urothelial neoplasm of low malignant potential (PUNLMP) may also arise from urothelium of bladder (1,2). The urothelium of a patient with a bladder cancer is at risk as the cancer often recurrs in the urinary bladder following treatment (1,3). Numerous genetic and epigenetic factors have been implicated in the carcinogenesis of the urinary bladder that involved in its mutator phenotype (4-7). The DNA repair mechanism is essential to prevent DNA mutations that may be lethal for cells (8). Mismatch repair (MMR) genes encode a number of DNA repair enzymes that cooperate to recognize and repair DNA mismatches (8,9). These enzymes act as complexes. A crucial complex that recognizes base-base mismatches is the MutSα, which consists of MSH2 and MSH6 components. MutLα is another MMR complex, consisting of MLH1 and PMS2 components that cooperate with MutSα and other enzymes to repair the damage (10-14). DNA repair dysfunction may allow the generation of a high-risk urothelium for malignant transformation in the urinary bladder. The dysfunction of MMR genes may present as an absence or reduction of MMR gene expression or microsatellite instability (MSI) phenotype (15-17). The protein expression levels of the *hMSH2*, *hMLH1* and *hMSH6* MMR genes have been detected in histopathological material of UCC specimens by immunohistochemistry (IHC) with controversial results (17-24). There is little and insufficient literature concerning the expression of the mRNA of MMR genes in bladder cancer specimens (25,26). In the present

study, we evaluated for the first time, by a precise quantitative real-time PCR (qPCR) analysis, the mRNA expression levels of the *hMSH2*, *hMLH1*, *hMSH6* and *hPMS2* MMR genes in surgical samples of bladder tumors paired with their corresponding adjacent normal tissues (ANTs). We also present the MMR phenotypes of reduced or elevated mRNA expression that were correlated with a high risk of malignant transformation of urothelium and/or tumor progression in the urinary bladder.

Materials and methods

Tissue collection and patients. Paired surgical specimens from primary bladder tumors and their ANTs were collected from 25 unselected patients who underwent surgery in the University Hospital of Alexandroupolis, Greece, after obtaining informed consent. The Ethics Committees of the University of Thessaly, Department of Pathology, Medical School of Larissa, Larissa, Greece and the Democritus University of Thrace, Departments of Urology and Pathology and University Hospital of Alexandroupolis, Alexandroupolis, Greece approved this study.

The clinical material was frozen at -80˚C and further subdivided for standard histological evaluation, DNA and RNA extraction. Tumor content >80% was recorded in all specimens studied. The histological review according to conventional guidelines (WHO/ISUP classification) revealed 24 UCCs and one PUNLMP in our clinical material. The UCCs further revealed 13 low grade tumors (6 in stage pT_a and 7 in pT_1) and 11 high grade tumors (1 in stage pT_a, 9 in pT_1 and 1 in pT_2; Table I).

The cohort of patients included 20 males and 4 females with UCC and 1 male with a PUNLMP with an age range of 50-90 years (median, 74; Table I).

Quantitative analysis of mRNA expression. We used Purescript® RNA isolation and SuperScript First Stand Synthesis System (Invitrogen®, Life Technologies, Paisley, UK) for cDNA synthesis, by reverse transcription (RT), as described previously (27). qPCR analysis of *hMSH2* and *hMLH1* mRNA was performed as previously described (16). qPCR analysis of *hMSH6* and *hPMS2* was performed using specific primers: *hMSH6* sense, 5'-AACAAGGGGCTGGGTTAG-3'; *hMSH6* antisense, 5'-CGTTGCATTGCTCTCAGTATTTC-3'; *hPMS2* sense, 5'-GAGTCAAGCAGATGTTTGCCTC-3'; *hPMS2* antisense, 5'-TGTGTCTCATGGTTGGCCTT-3'; and fluorescent hybridization probes *hMSH6*-FL, 5'-TATACA GGTTCAAAATCAAAGGAAGCCC-FL; *hMSH6*-LC, 5'-LC640-GAAGGGAGGTCATTTTTACAGTGCAAG-PH; *hPMS2*-FL, 5'-GGGTGATCAGTTTCTTCATCTCGC TTGT-FL; *hPMS2*-LC, 5'-LC640-TTAAGAGCAGTCCCA ATCATCACCGACTT-PH designed for Light Cycler instrument 3.5 (TIB® Molbiol, Berlin, Germany). All reactions included Porphobilionogen deaminase (*hPBGD*) housekeeping gene primers as internal controls (Roche Diagnostics, Mannheim, Germany). Following an initial denaturation step at 95˚C for 10 min, *hMSH6*-PCR assays underwent 45 cycles of denaturation at 95˚C for 10 sec, annealing at 54.2˚C for 15 sec and extension at 72˚C for 6 sec and *hPMS2*-PCR assays underwent 45 cycles of denaturation at 95˚C for 10 sec, annealing at 57˚C for 10 sec and extension at 72˚C for 6 sec. The mRNA expression of each MMR gene was expressed as a ratio of MMR gene mRNA to control *hPBGD* mRNAs (MMR/control mRNAs) and defined two major phenotypic groups, the reduced (r) for mRNA ratios <1 and the normal or elevated (R) for ratios ≥1, as previously described (16). Additionally, the MMR gene expression of tumor samples was compared with that of the corresponding ANT samples. This value is indicated as relative mRNA expression of MMR genes between tumor and ANT (tumor/ANT) of each patient (Table I).

Genomic instability analysis. Genomic instability analysis was performed for the following polymorphic regions of the *hMSH2* and *hMLH1* loci: *D3S1234* (3p14), *D3S1612* (3p21.3-22) and *D3S1768* (3p21.3-22) distal to the *hMLH1* locus on chromosome 3p and *D2S1788* (2p22.3) proximal to the *hMSH2* locus on chromosome 2p, to compare the possible loss of mRNA expression with allelic imbalance of the chromosomal regions that contain the genes (28). The primer sequences for each microsatellite copy were obtained from the National Center for Biotechnology Information database. Nucleotide repeat markers, stretches within non-coding repeats such as *BAT26* in intron 5 of *hMSH2* and *BAT25* in intron 16 of *c-kit* were used as established mononucleotide markers for determining MSI status (29,30).

MSI analysis was performed as previously described (31). Briefly, following DNA extraction from bladder tissue specimens (Puregene® Cell and Tissue extraction kit; Gentra), genomic DNA samples were stored at -20˚C until use. PCR analysis included amplification of the *β-globin* gene in order to qualify and normalize the amount of DNA in each sample. The primers used for the amplification of the *β-globin* gene, PCR, qPCR and melting curve analysis conditions were as previously described (31). All samples were run in duplicate and two non-template-controls (NTCs) were included in the reactions. qPCR amplifications and melting curve analyses were repeated twice. The conditions of reactions were 95˚C for 15 min, 36 cycles of 95˚C for 15 sec, annealing temperature for each set of primers (55˚C for *D3S1768*, *D2S1788*, *BAT25*; 56˚C for *D3S1612*; 56.5˚C for *BAT26*; and 58.5˚C for *D3S1234*) for 30 sec and 72˚C for 30 sec (acquiring for SYBR). Continuously Melting Curve analysis performed ramping 65-95˚C (raising by 0.2˚C each step) and finishing at 72˚C for 5-10 min. Following completion of the amplification melting curve, analysis was performed as previously described (31).

Statistical analysis. We used the paired Student's t-test to compare ratios of *hMSH2*, *hMLH1*, *hMSH6* and *hPMS2* alterations between tumor and matched ANT for different patient characteristics, including age, gender and clinicohistopathological parameters such as tumor type, grade and stage. The correlation between the mRNA expression ratios of *hMSH2*, *hMLH1*, *hMSH6* and *hPMS2* in bladder tumors and their ANTs for different patient and tumor characteristics was examined by Pearson test. The χ^2 test was also used to examine the distribution of MMR mRNA phenotypes (r, R, rr, rR, Rr and RR) in tumor and ANT specimens at different tumor histopathological grades or stages. Statistical significance was considered for values of $p<0.05$.

Table I. Quantitative mRNA expression of *hMSH2*, *hMLH1*, *hMSH6* and *hPMS2* in bladder tumors and their adjacent normal tissue.

Patient no./age (years)/ gender	Tumor type	Tumor grade	pTNM classification	*hMSH2*/ *control* mRNA[a]		*hMLH1*/ *control* mRNA[a]		*hMSH6*/ *control* mRNA[a]		*hPMS2*/ *control* mRNA[a]		Tumor/ANT MMR mRNA expression[b]			
				Tumor	ANT	Tumor	ANT	Tumor	ANT	Tumor	ANT	*hMSH2*	*hMLH1*	*hMSH6*	*hPMS2*
1/70/M	PUNLMP	-	pT_a	0.46	2.9	0.22	0.24	0.74	1.1	1.59	3.87	0.16	0.92	0.67	0.4
2/50/M	UCC	LG	pT_a	10.2	1.58	14.7	4.6	90	16	24.4	7.8	6.5	3.2	5.6	3
3/59/M	UCC	LG	pT_a	3.2	0.73	5.6	1.3	8.64	15.4	13.25	26.52	4.4	0.56	0.5	4.3
4/73/M	UCC	LG	pT_a	2	0.82	12	4.45	1.7	0.88	1.7	1.67	2.4	1.9	0.8	2.7
5/75/M	UCC	LG	pT_a	4.12	2.9	8.29	19.25	59	47	8.3	16.82	1.97	0.43	1.24	0.4
6/75/M	UCC	LG	pT_a	1.26	6.22	8	7.7	21.9	64	24.3	15.8	0.2	1.04	0.34	1.5
7/79/F	UCC	LG	pT_a	1.56	1.14	2.58	2.26	2.27	1.9	4.7	1.5	1.36	1.19	3	1.13
8/56/M	UCC	LG	pT_1	0.4	0.54	1.89	2.4	0.44	0.55	0.86	0.83	0.73	0.8	1	0.79
9/69/M	UCC	LG	pT_1	1.66	0.6	2.65	1.96	0.9	0.6	1.1	0.69	2.8	1.5	1.6	1.4
10/69/M	UCC	LG	pT_1	1.22	0.88	8.76	4.72	2.5	0.8	2.5	1.8	1.39	3.13	0.13	1.86
11/73/F	UCC	LG	pT_1	9.4	23.5	38	38	3.2	3.4	5.9	5.9	0.4	1	1	1
12/76/M	UCC	LG	pT_1	3.97	1.43	5.4	2.49	1.73	0.76	7.29	136.27	2.8	2.28	0.5	2.2
13/82/M	UCC	LG	pT_1	7.5	13.8	28	25	1.8	1.68	17.8	7.14	0.5	1	0.2	1.12
14/82/M	UCC	LG	pT_1	1.8	1.45	1.87	2.36	2.2	2.4	2.29	2.78	1.3	0.9	0.8	0.79
15/72/F	UCC	HG	pT_a	0.74	0.5	2.38	4.25	0.62	0.47	0.7	0.57	1.48	1.3	1.2	0.56
16/54/M	UCC	HG	pT_1	3.1	1	5.58	2.26	5.8	0.79	37.8	20.39	2.6	6.8	1.85	2.5
17/62/M	UCC	HG	pT_1	3.78	4.29	25.73	15.78	39.7	63.4	27.4	21.4	0.87	1.6	0.6	1.6
18/75/M	UCC	HG	pT_1	8	0.55	2.83	2.31	5.4	1	47.6	16	14.55	5.4	2.9	1.22
19/76/M	UCC	HG	pT_1	0.49	0.7	1.65	1.8	0.73	2.2	2.3	9.8	0.57	0.33	5	0.9
20/83/M	UCC	HG	pT_1	1.4	0.4	3	5.7	2.5	2.2	3.8	5.6	3.5	1.14	0.7	0.53
21/84/M	UCC	HG	pT_1	0.75	0.6	1.42	1.67	0.87	0.67	1.12	6.5	1.2	1.3	0.17	0.85
22/90/F	UCC	HG	pT_1	0.16	1.03	1.08	2.6	0.12	0.65	0.8	104	0.15	0.19	0.001	0.4
23/72/M	UCC	HG	pT_1	21.66	5	20	12.3	130	59	37	24.7	4.3	14	2.2	1.5
24/75/M	UCC	HG	pT_2	1.63	0.7	7	2.1	2.19	0.74	35.7	1.8	2.3	2.9	19.9	3.3
25/68/M	UCC	HG	pT_1	NA	NA	NA	NA	0.37	NA	11.5	NA	-	-	-	-

ANT, adjacent normal tissue; MMR, mismatch repair; M, male; F, female; PUNLMP, papillary urothelial neoplasm low malignant potential; UCC, urothelial cell carcinoma; LG, low grade; HG, high grade; pT_a, limited to mucosa; pT_1, lamina propria invasion; pT_2, invasion of the muscularis; NA, non-amplified sample. [a]Ratios of mRNA expression; [b]ratios of tumor to ANT mRNA expression.

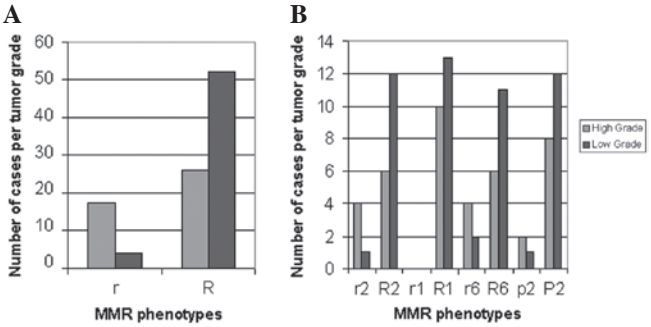

Figure 1. (A) Relative distribution of reduced (r/p) to normal or elevated (R/P) MMR phenotypes to histological tumor grades in UCCs. (B) Relative distribution of each *hMSH2* (r_2/R_2), *hMLH1* (R_1), *hMSH6* (r_6/R_6) and *hPMS2* (p_2/P_2) mRNA phenotypes to histological tumor grades in UCCs. MMR, mismatch repair; UCC, urothelial cell carcinoma.

Results

hMSH2, hMLH1, hMSH6 and hPMS2 mRNA quantification in bladder tumors. We evaluated *hMSH2*, *hMLH1*, *hMSH6* and *hPMS2* mRNA levels in primary UCCs and their corresponding ANTs relative to the reference *hPBGD* control gene by qPCR (Fig. 1). These data are summarized in Table I with patient age, gender, tumor type, stage and grade.

The urothelium adjacent to UCCs revealed reduced mRNA ratios (<1) of the *hMSH2*, *hMSH6* and *hPMS2* genes in 47.8 (11/23), 43.5 (10/23) and 13% (3/23) of samples, respectively, compared with 21.7 (5/23), 29.2 (7/24) and 12.5 (3/24) of UCC tumors (P=0.027284). We observed a statistically significant difference between the proportions of reduced mRNA ratios of *hMSH2*/*control* and *hMSH6*/*control* genes observed in ANTs of low grade UCCs relative to their tumors (P=0.025347) that was more pronounced than those observed between ANTs and high grade UCCs (P=0.000; Table I). Moreover, high grade UCCs exhibited higher proportions of reduced mRNA ratios of *hMSH2*/*control*, *hMSH6*/*control* and *hPMS2*/*control* (40, 40 and 20%, respectively) compared with low grade tumors (7.6, 15.3 and 7.6%, respectively; P=0.000).

The *hMLH1*/*control* mRNA ratios were ≥1 in UCCs and their ANTs, contrary to PUNLMP and its corresponding ANT that exhibited reduced mRNA ratios (<1). PUNLMP also showed reduced (<1) *hMSH2*/*control* and *hMSH6*/*control* mRNA ratios, while its corresponding ANT exhibited elevated or normal (≥1) ratios.

hMSH2, hMLH1, hMSH6 and hPMS2 mRNA relative expression. Calculation of tumor/ANT MMR mRNA ratios from quantification data (Table I) revealed different proportions of UCC ratios ≤0.8 with 26.1% (6/23) for *hMSH2*, 21.7% (5/23) for *hMLH1*, 47.8% (11/23) for *hMSH6* and 26% (6/23) for *hPMS2*, respectively. Calculation of PUNLMP/ANT MMR mRNA revealed ratios ≤0.8 of *hMSH2*, *hMSH6* and *hPMS2* (Table I). The reduction in *hMSH2*, *hMLH1*, *hMSH6* and *hPMS2* mRNA expression between primary bladder tumors and their matched ANTs, male and female, pT_a stage and pT_1, high and low grade UCC was not statistically significant by paired Student's t-test analysis (Table II).

Bladder tumors revealed mRNA overexpression ratios (≥1.8) of *hMSH2*, *hMLH1*, *hMSH6* and/or *hPMS2* compared with their corresponding ANTs in 47.8 (11/23), 35 (8/23), 30 (7/23) and 30% (7/23) of specimens, respectively (Table I).

The statistically significant difference of *hMSH2* transcriptional levels between UCC tumors and their matched ANTs (P=0.019165; Student's t-test) was more pronounced in males compared with females (males, P=0.020265; females, P=0.169501; Student's t-test) and was independent of stage (pT_a, P=0.127745; pT_1, P=0.089642; Student's t-test; Table II). Low grade UCCs exhibited a statistically significant elevation of *hMSH2* mRNA expression relative to their matched ANTs (low grade, P=0.048544; high grade, P=0.130441; Student's t-test; Table II).

We observed significant difference in *hMLH1* transcriptional activation between bladder tumors and their matched ANTs (P=0.000; Student's t-test; Table II). Notably, males showed a higher *hMLH1* transcriptional activation in tumors compared with females (males, P=0.000366; females, P=0.5; Student's t-test; Table II). We also observed statistically significantly higher levels of *hMLH1* mRNA expression between UCC tumors and their matched ANTs of pT_1 stages than pT_a (pT_1, P=0.012455; pT_a, P=0.081273; Student's t-test; Table II). Low grade UCCs compared with their matched ANTs exhibited relatively higher mRNA expression levels of *hMLH1* than high grade UCCs (low grade, P=0.012; high grade, P=0.032; Student's t-test; Table II).

The statistically significantly elevated mRNA expression of *hPMS2* observed between UCC tumors and their matched ANTs (P=0.005896; Student's t-test) was also identified in males compared with females (males, P=0.005159; females, P=0.474152; Student's t-test), pT_1 UCCs (pT_1, P=0.038387; pT_a, P=0.143226; Student's t-test) and was pronounced in high grade compared with low grade tumors (high grade, P=0.028778; low grade, P=0.05819; Student's t-test; Table II).

Correlation between mRNA expression of the hMSH2, hMLH1, hMSH6 and hPMS2 MMR genes in bladder tumors. We observed a statistically significant correlation between *hMSH2*/*hPBGD* and *hMSH6*/*hPBGD* mRNA ratios in bladder tumors (r=0.795; Pearson test; Table II).

We also observed a statistically significant association between the relative mRNA expression of *hMSH2* and *hMLH1* (tumor/ANT) expression (r=0.415684; Pearson test) that was more pronounced in females compared with males (females, r=0.873155; males, r=0.37; Pearson test), slightly more intense in pT_a than pT_1 stages (pT_a, r=0.778713; pT_1, r=0.61326; Pearson test) and in low grade than high grade UCCs (low grade, r=0.700724; high grade, r=0.598678; Pearson test; Table II). Only females exhibited a statistically significant association of relative mRNA expression between *hMSH2* and *hMSH6* (r=0.735679, Pearson test), *hMLH1* and *hPMS2* (r=0.560746; Pearson test) and *hMSH6* and *hPMS2* (r=0.801165; Pearson test; Table II). In addition, females and pT_a UCCs exhibited a significant association between *hMLH1* and *hMSH6* relative (tumor/ANT) levels of mRNA expression (female, r=0.728012; pT_a, r=0.567703; Pearson test; Table II).

Phenotyping MMR sorting. We used the ratio of MMR mRNA expression relative to reference mRNA control to adopt a functional unified assessment for our findings, as previously described (16). We classified our specimens into two major

Table II. Alterations of *hMSH2*, *hMLH1*, *hMSH6* and *hPMS2* mRNA levels between paired bladder tumor and adjacent normal tissues relative to their clinicopathological parameters.

Characteristics	n	Relative copies of *hMSH2* mRNA		Relative copies of *hMLH1* mRNA		Relative copies of *hMSH6* mRNA		Relative copies of *hPMS2* mRNA		Tumor/ANT MMR mRNA gene expression			
		Tumor	ANT	Tumor	ANT	Tumor	ANT	Tumor	ANT	*hMSH2*	*hMLH1*	*hMSH6*	*hPMS2*
All patients	24	3.77[a,b]	3.06	8.69[e]	7	16	12	12.9[j]	18.34	2.4[n]	2.4	2.19	1.52
Gender													
Male	20	3.93[c]	2.37	8.23[f]	6	19	14	14.9[k]	16.41	2.75[o]	2.79	2.43	1.68
Female	4	2.96	6.54	11	12	1.6	1.6	3.03	28	0.85[p,v]	0.9[w,y]	1.3[z]	0.77
Tumor type													
PUNLMP	1	0.46	2.9	0.22	0.2	0.74	1.1	1.59	3.87	0.16	0.67	0.4	0.9
UCC	23	3.9	3.07	9.06	7.3	16.7	12.5	13.42	18.97	2.5[q]	2.66	2.33	1.55
Tumor stage													
T_a	7 (6LG+1HG)	3.3[d]	1.98	7.65	6.26	26.3	20.8	11.05	10.1	2.62[r]	1.73[x]	1.5	2.8
T_1	15 (7LG+8HG)	4.35	3.73	9.86[g]	8.09	13.13	9.34	13.04[l]	24.25	2.51[s]	1.89	1.24	2.07
T_2	1 (HG)	1.63	0.7	7	2.1	2.19	0.74	35.7	1.8	2.3	2.9	19.9	3.3
Tumor grade													
LG	13 ($6T_a$+$7T_1$)	3.71	4.27	10.6[h]	8.96	15.1	12	8.8	17.35	2.06[t]	1.64	1.11	2.17
HG	10 ($1T_a$+$9T_1$)	4.17	1.5	7.07[i]	5.08	18.79	13.1	19.42[m]	21.08	3.15[u]	2.21	3.45	2.59

Mean age of the patients was 72 years. ANT, adjacent normal tissue; MMR, mismatch repair; PUNLMP, papillary urothelial neoplasm of low malignant potential; UCC, urothelial cell carcinoma; LG, low grade; HG, high grade. [a]r=0.795, by Pearson test; correlation between *hMSH2*/*hPBGD* and *hMSH6*/*hPBGD* mRNA ratios. [b]P=0.019165, [c]P=0.020265, [d]P=0.048544, [e]P=0.000, [f]P=0.000366, [g]P=0.012455, [h]P=0.012, [i]P=0.032, [j]P=0.005896, [k]P=0.005159, [l]P=0.038387, [m]P=0.028778; by Student's t-test. [n]r=0.415684, [o]r=0.37, [p]r=0.873155, [q]r=0.44, [r]r=0.778713, [s]r=0.613262, [t]r=0.700724, [u]r=0.598678; by Pearson test, correlation between *hMSH2* and *hMLH1* mRNA ratios of tumor/ANT. [v]r=0.735679 by Pearson test, correlation between *hMSH2* and *hMSH6* mRNA ratios of tumor/ANT. [w]r=0.728012, [x]r=0.567703 by Pearson test, correlation between *hMLH1* and *hMSH6* mRNA ratios of tumor/ANT. [y]r=0.560746 Pearson test, correlation between *hMLH1* and *hPMS2* mRNA ratios of tumor/ANT. [z]r=0.801165 Pearson test, correlation between *hMSH6* and *hPMS2* mRNA ratios of tumor/ANT.

Table III. Distribution of individual *hMSH2*, *hMLH1*, *hMSH6* and *hPMS2* mRNA phenotypes in UCCs and their ANTs.

MMR mRNA phenotype	UCC (n)	UCC observed phenotypic frequency	Grade (n)		Stage (n)		ANT (n)	ANT observed phenotypic frequency	Samples (n)	
			LG	HG	pT_a	pT_{1-2}			PUNLMP	ANT
hMSH2										
r_2	5	0.2174	1	4	1 (HG)	4 (1LG+3HG)	11	0.4783	1	
R_2	18	0.7826	12	6	6 (LG)	12 (6LG+6HG)	12	0.5217		1
hMLH1										
r_1	0	0.000	0	0	0	0	0	0.000	1	1
R_1	23	1.000	13	10	7 (1LG+6HG)	16 (7LG+9HG)	23	1.000		
hMSH6										
r_6	6	0.2609	2	4	1 (HG)	5 (2LG+3HG)	10	0.4348	1	
R_6	17	0.7391	11	6	6 (LG)	11 (5LG+6HG)	13	0.5652		1
hPMS2										
p_2	3	0.1304	1	2	1 (HG)	2 (1LG+1HG)	3	0.1304		
P_2	20	0.8696	12	8	6 (LG)	14 (6LG+8HG)	20	0.8696	1	1

ANT, adjacent normal tissue; MMR, mismatch repair; UCC, urothelial cell carcinoma; LG, low grade; HG, high grade; PUNLMP, papillary urothelial neoplasm of low malignant potential; pT_a, limited to mucosa; pT_1, lamina propria invasion; pT_2, invasion of the muscularis; r/p, reduced, mRNA ratio <1; R/P, normal/elevated, mRNA ratio ≥1; r/R_2, *hMSH2*; r/R_1, *hMLH1*; r/R_6, *hMSH6*; p/P_2, *hPMS2*.

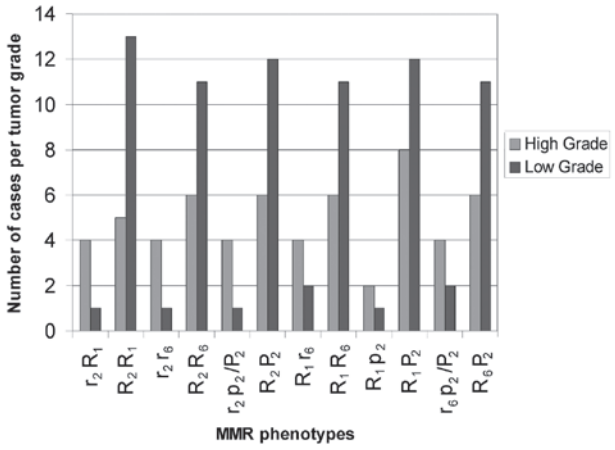

Figure 2. Relative distribution of combined *hMSH2*, *hMLH1*, *hMSH6* and *hPMS2* mRNA phenotypes to histological tumor grades in UCCs. r/p, reduced, mRNA ratio <1; R/P, normal/elevated, mRNA ratio ≥1; r/R_2, *hMSH2*; r/R_1, *hMLH1*; r/R_6, *hMSH6*; p/P_2, *hPMS2*; MMR, mismatch repair; UCC, urothelial cell carcinoma.

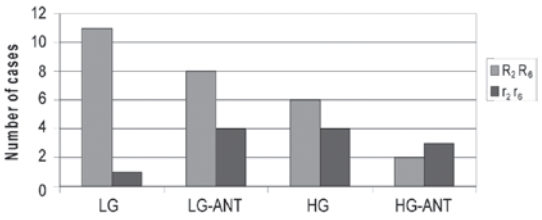

Figure 3. Relative distribution of cases with combined reduced (r_2r_6) or normal or elevated (R_2R_6) *hMSH2* and *hMSH6* mRNA phenotypes to low or high grade UCCs (LG, HG) and their matched ANTs (LG-ANT, HG-ANT). UCC, urothelial cell carcinoma; ANT, adjacent normal tissue.

phenotypic groups, one with reduced (r) and the other with regular or enhanced (R) ratios of expression (Materials and methods) and subdivided our study group into eight phenotypes, r_2 and R_2 for *hMSH2*, r_1 and R_1 for *hMLH1*, r_6 and R_6 for *hMSH6* and finally p_2 and P_2 for *hPMS2* DNA repair system components (Table III) or their combined phenotypes R_2R_1, R_2R_6, R_2P_2, R_1R_6, R_1P_2, R_6P_2 and R_2r_1, R_2r_6, R_2p_2, R_1r_6, R_1p_2, R_6p_2 and r_2R_1, r_2R_6, r_2P_2, r_1R_6, r_1P_2, r_6P_2 and r_2r_1, r_2r_6, r_2p_2, r_1r_6, r_1p_2, r_6p_2 by descending MMR system activity.

Clinical and biological evaluation of single and combined MMR phenotypic distributions. We tested the ability of our phenotypes to distinguish our study group into distinct bladder tumors and ANTs subtypes. We thus examined the significance of the differences between the subgroups created according to our phenotypic criteria (Table III, Fig. 1).

The distribution of individual r and R MMR mRNA phenotypes was significantly different between ANTs and UCCs (P=0.021751; χ^2 test), particularly r_2 vs. R_2 (P=0.012261; χ^2 test). Additionally, a marked difference of r and R phenotypic distribution was observed between high and low grade UCCs (P=0.00013; χ^2 test; Fig. 1A), particularly r_2 vs. R_2 (P=0.00053, χ^2 test) and r_6 vs. R_6 (P<0.04, χ^2 test; Fig. 1B). The frequencies of independent r_2, r_1, r_6, p_2, R_2, R_1, R_6 and P_2 phenotypes in UCCs and their corresponding ANTs are shown in Table III. The reduced r_1 phenotype was not identified in any UCC or corresponding ANTs, in contrast to the PUNLMP and its ANT (Table III).

The distribution of combined MMR mRNA phenotypes in UCCs and their matched ANTs are shown in Table IV. We observed two r_2R_1 and R_2R_1 combined *hMSH2* and *hMLH1* mRNA phenotypes, two R_1p_2 and R_1P_2 combined *hMLH1* and *hPMS2* phenotypes and two R_1r_6 and R_1R_6 combined *hMLH1* and *hMSH6* mRNA phenotypes in UCCs and/or their ANTs with same frequencies between observed and calculated frequencies of combined loci. We also observed four R_2R_6,

Table IV. Distribution of combined *hMSH2*, *hMLH1*, *hMSH6* and *hPMS2* mRNA phenotypes in UCCs and their ANTs.

Tissue	R_2R_1	r_2R_1	R_2r_1	r_2r_1	R_6P_2	r_6P_2	r_6p_2	R_6p_2	R_2R_6	r_2R_6	R_2r_6	r_2r_6
UCCs	18	5	0	0	17	3	3	0	17	0	1	5
Observed frequencies	0.7826	0.2714	0.000	0.000	0.7391	0.1304	0.1304	0.0000	0.7391	0.000	0.0435	0.2174
Calculated phenotypic frequencies of combined loci	0.7826	0.2714	0.000	0.000	0.6427	0.2269	0.0340	0.0964	0.5784	0.2006	0.2042	0.0708
Grade												
LG	13	1	0	0	11	1	1	0	11	0	1	1
HG	5	4	0	0	6	2	2		6	0	0	4
Stage												
pT_a	6	1	0	0	6	0	1	0	6	0	0	1
pT_{1-2}	12	4	0	0	11	3	2	0	11	0	1	4
ANT	14	9	0	0	14	6	3	0	10	4	4	5
Observed frequencies	0.6087	0.3913	0.000	0.000	0.6087	0.2609	0.1304	0.000	0.4348	0.1739	0.1739	0.2174
	R_2P_2	r_2P_2	R_2p_2	r_2p_2	R_1P_2	r_1P_2	R_1p_2	r_1p_2	R_1R_6	r_1R_6	R_1r_6	r_1r_6
UCCs	18	2	0	3	20	0	3	0	17		6	0
Observed frequencies	0.7826	0.087	0.0000	0.1304	0.8696	0.000	0.1304	0.000	0.7391	0.000	0.2609	0.000
Calculated phenotypic frequencies of combined loci	0.6806	0.236	0.1021	0.0354	0.8696	0.000	0.1304	0.000	0.7391	0.000	0.2609	0.000
Grade												
LG	12	0	0	1	12	0	1	0	11	0	2	0
HG	6	2	0	2	8	0	2	0	6	0	4	0
Stage												
pT_a	6	0	0	1	6	0	1	0	6	0	1	0
pT_{1-2}	12	2	0	2	14	0	2	0	11	0	5	0
ANT	14	6	0	3	20	0	3	0	14	0	9	0
Observed frequencies	0.6087	0.2609	0.000	0.1304	0.8696	0.000	0.1304	0.000	0.6087	0.000	0.3913	0.000

UCC, urothelial cell carcinoma; ANT, adjacent normal tissue; LG, low grade; HG, high grade; pT_a, limited to mucosa; pT_1, lamina propria invasion; pT_2, invasion of the muscularis; r/p, reduced, mRNA ratio <1; R/P, normal/elevated, mRNA ratio ≥1; r/R_2, *hMSH2*; r/R_1, *hMLH1*; r/R_6, *hMSH6*; p/P_2, *hPMS2*.

Table V. Genetic alterations in UCCs using melting curve analysis.

Case no., T/N	Polymorphic markers at the 3p loci (distal to *hMLH1*)					Polymorphic markers at the 2p loci (within or distal to *hMSH2*)				Polymorphic marker related to MSI
	D3S1234	*D3S1768*		*D3S1612*		*BAT26*	*D2S1788*			*BAT25*
	[a]Peak	Peak 1	Peak 2	Peak 1	Peak 2	Peak 1	Peak 1	Peak 2	Peak 3	Peak 1
1										
T	77.7		73.5	75.6	76.2	73.8	73.5			72.5
N	77.8		73.7	75.6	76.2	73.8	73.5			72.5
2										
T	NA		NA	NA		NA	NA			NA
N	NA		NA	NA		NA	NA			NA
3										
T	77		73.3		76.4	73.7	NA			72.6
N	77		73.3		NA	NA	NA			72.5
4										
T	76.8		73		76.4	73.7	72.3	73.5		NA
N	76.7		73.3	75.5	76.2	73.9	NA	NA		NA
5										
T	NA		NA	NA		NA	NA			NA
N	NA		NA	NA		NA	NA			NA
6										
T	NA		NA	NA		NA	NA			NA
N	NA		NA	NA		NA	NA			NA
7										
T	77.5		73.5	75.7	76.3	73.7	73.5			72.75
N	77.5		73.5	75.7	76.3	73.7	73.5			72.75
8										
T	77.4		73.3	75.6		73.7	73.4			72.8
N	77.5		73.5	75.6		73.7	73.4			72.8
9										
T	77.6		73.2		76.4	73.8	73.5	74.5		72.7
N	77.5		73.5		76.4	73.8	73.5	74.5		72.6
10										
T	76.8		73.66	NA		NA	73	74.2		73
N	76.8		73.70	NA		NA	73	74.2		73.2
11										
T	77.7		73.4		77.1	73.3	73.4		76.8	NA
N	77.7		NA		77.2	NA	NA		NA	NA
12										
T	76.7		NA	NA		73.7	NA			NA
N	76.5		NA	NA		73.7	NA			NA
13										
T	77.5		73.5	76.4		73.8	73.4		76.8	NA
N	77.5		NA	76.4		NA	NA		NA	NA
14										
T	77.4		73.2		76.9	73.7	73.4		76.6	72.55
N	77.4		73.2		77	73.7	73.4		76.6	72.65
15										
T	78.1		NA	75.7	76.8	73.7	73.5		76.6	72.8
N	78.1		73.5	75.7	76.9	73.7	73.4		76	72.9
16										
T	77.4		73.5	75.5	76.7	73.9	NA			72.4
N	77.3		73.64	75.5	76.7	73.9	NA			72.8

Table V. Continued.

Case no., T/N	Polymorphic markers at the 3p loci (distal to *hMLH1*)					Polymorphic markers at the 2p loci (within or distal to *hMSH2*)				Polymorphic marker related to MSI
	D3S1234	*D3S1768*		*D3S1612*		*BAT26*	*D2S1788*			*BAT25*
	[a]Peak	Peak 1	Peak 2	Peak 1	Peak 2	Peak 1	Peak 1	Peak 2	Peak 3	Peak 1
17										
T	NA		NA	NA		NA	NA			NA
N	NA		NA	NA		NA	NA			NA
18										
T	77.8		73.6		76.5	73.7	NA			72.3
N	77.7		NA		76.5	73.7	NA			72.6
19										
T	77.5		73.4	75.6	76.9	73.7	73.4		75.7	72.7
N	77.5		73.7	75.6	76.9	73.7	NA		NA	73.2
20										
T	77.3		73.5		76.5	73.7	73.5			72.5
N	77.2		NA	75.6	76.5	73.7	73.5			72.5
21										
T	78.2		73.5		76.6	NA	NA			NA
N	NA		NA		76.5	NA	NA			NA
22										
T	77		73.76		NA	NA	NA			NA
N	77		73.70		NA	NA	NA			73.2
23										
T	NA		NA		NA	NA	NA			NA
N	NA		NA		NA	NA	NA			NA
24										
T	77.2		NA		76.6	73.7	73.3		76	72.5
N	77		NA		76.4	73.8	73.5		76	72.6
25										
T	77.5	72.7	73.7		77.2	73.8	73.4		76.6	72.9
N	77.5		73.7		77.1	73.8	NA		NA	72.9

[a]Melting temperature peaks of polymorphic markers. Genotyping, heterozygous samples (two peaks), homozygous (one peak). NA, non-amplified sample. Genetic alterations: LOH, loss of heterozygosity, shown as loss of a melting peak temperature in tumor tissue sample (cases 4 and 20, loss of peak 1/*D3S1612* locus); MSI, microsatellite instability, shown as creation of a new melting peak in tumor tissue sample (case 25, new peak 1/*D3S1768* locus). UCC, urothelial cell carcinoma; T, tumor; N, normal.

r_2R_6, R_2r_6 and r_2r_6 combined *hMSH2* and *hMSH6*, three R_2P_2, r_2P_2 and r_2p_2 combined *hMSH2* and *hPMS2* and three R_6P_2, r_6P_2 and r_6p_2 combined *hMSH6* and *hPMS2* mRNA phenotypes in UCCs and/or their ANTs with different frequencies between observed and calculated frequencies of combined loci. There was a statistically significant difference between high and low grade tumors in r_2R_1 vs. R_2R_1 ($P=0.00019$; χ^2 test), r_2r_6 vs. R_2R_6 ($P=0.000786$; χ^2 test), r_2p_2/P_2 vs. R_2P_2 ($P=0.00053$, χ^2 test) and less marked in R_1r_6 vs. R_1R_6 ($P<0.04$; χ^2 test) and in r_6p_2/P_2 vs. R_6P_2 ($P<0.04$, χ^2 test). The histogram in Fig. 2 shows the association of reduced (homozygous or heterozygous) r_2R_1 or r_2r_6 or r_2p_2/P_2 or R_1r_6 or r_6p_2/P_2 and normal or elevated (homozygous) R_2R_1 or R_2R_6 or R_2P_2 or R_1R_6 or R_6P_2 to high and low grades, respectively (Table IV and Fig. 2).

A statistically significant difference was also observed between R_2R_6 and r_2r_6 phenotypic distribution in UCCs relative to their ANTs ($P<0.02$; χ^2 test) that was pronounced in low compared with high grade tumors ($P=0.0000006$; χ^2 test; Table IV and Fig. 3).

Genomic instability. We examined 6 genetic markers for genomic instability [MSI and/or loss of heterozygosity (LOH)] in bladder tumors (Table V) distal or close to *hMLH1* and *hMSH2* to determine the correlation between possible loss of mRNA expression and allelic imbalance of the chromosomal regions that harbor the genes. *D2S1788* (2p22.3) and *BAT26* are located distal to and in the *hMSH2* locus, respectively, while *D3S1612* (3p21.3-22), *D3S1768* (3p21.3-22) and *D3S1234*

(3p14) are distal to the *hMLH1* locus. Additionally, *BAT25* stretches within the *c-kit* gene and was included as it has been previously correlated with a DNA repair mechanism (29,30).

We observed genetic instability (MSI and/or LOH) in 3 (15%) of the 20 analyzed bladder tumors vs. their ANTs. Two polymorphic regions at the 3p loci had been affected (distal to *hMLH1*). *D3S1768* locus exhibited MSI in one of the 12 (8.3%) analyzed cases, which was characterized as MSI-L (one unstable marker), while the remaining cases were not informative for LOH (Table V). *D3S1612* locus was affected by LOH in two out of 7 (28.57%) informative cases (Table V). None of the MSI-analyzed cases were informative for LOH at the *D3S1234*, *D3S1788*, *BAT25* or *BAT26* polymorphic regions (Table V).

The MSI-L bladder tumor was a high grade UCC with stage pT_1, while LOH was noted in a low grade pT_a stage and a high grade pT_1 stage UCC. The 2 UCCs which showed LOH at the *D3S1612* (3p21.3-22) locus exhibited normal or elevated MMR phenotypes but reduced (≤0.8) *hMSH6* mRNA tumor/ANT ratios (Tables I and V).

Discussion

To date, a series of studies have attempted to determine the expression of MMR proteins, mainly MSH2 and MLH1, in bladder cancer, the majority using IHC methods (17-24). Only two previous studies have determined MMR mRNA levels in bladder cancer by qPCR analysis and even in a few series of clinical specimens with different percentages from IHC analysis (25,26). The current study presents for the first time a quantification analysis of MMR mRNA transcripts in paired bladder tumors and their ANTs.

It is known that MSH2/MSH6 proteins form heterodimers that act as a complex (MutSα). This complex function is to detect single base-base mismatches and insertion-deletion loops and bind to the side of the DNA error (11,12,14). Our data showed that unaffected urothelia adjacent to UCC tumors (mainly adjacent to low grade UCC tumors) express low ratios of *hMSH2* and *hMSH6* mRNA levels (r_2r_6 phenotype), implying a low activity of DNA damage recognition of single mismatches and insertion-deletion loops errors. The ANTs of high grade UCCs also exhibited a reduced r_2r_6 phenotype, leaving the urothelium at high risk of cancer. Moreover, urothelia adjacent to high grade UCCs showed statistically higher percentages of the reduced r_2r_6 phenotype, approaching the levels of high grade tumors, in contrast to ANT of low grade UCCs, which showed a significant difference between the corresponding tumors. However, the *hMLH1* gene was found to have elevated mRNA ratios (R_1 phenotype) both in UCCs and their ANTs, indicating either high requirements for DNA repair of the progressively increasing errors in cancerous or precancerous urothelium or the involvement of *hMLH1* in another tumorigenesis pathway (33). The counterpart of *hMLH1*, *hPMS2*, was also overexpressed in a percentage of pT_{1-2} and high grade UCCs, to cooperate with MLH1 as complex (MutLα) due to the demanding repair or another function (10,14,34). Nevertheless, a percentage of UCCs presented reduced levels of *hMLH1* and *hPMS2* mRNA expression relative to their ANTs which indicates low DNA repair activity in a large proportion of UCCs and therefore accumulation of replication errors in the abnormal proliferating malignant cells.

The unbalanced mRNA levels of MMR genes, including overexpression of *hMSH2*, *hMLH1* and *hPMS2* and reduction of mRNA levels of *hMSH6*, in the urothelium of UCC, mainly in males, was correlated with tumor progression. A recent study implicates MutLα as a general stimulating factor for miRNA biogenesis, giving the complex an additional function in tumorigenesis (34). In our cohort of specimens we observed that a proportion of tumors exhibited mRNA overexpression of *hMSH2*, *hMLH1* and *hPMS2*. For *hMSH2* this was more frequent in low grade pT_a tumors; for *hMLH1* in low grade pT_1 tumors; and for *hPMS2* for high grade pT_{1-2} tumors relative to the ANTs that may indicate the tumor progression. An explanation may be that from low to high grade tumors or from pT_a to pT_3 histological stages additional DNA errors take place, e.g., small and larger insertion-deletion loops (12,13). The need for recognition of these errors by other MMR complexes and enzymes, such as MutSβ (MSH2-MSH3), is indicated by the significant reduction of the *hMSH6* counterpart of *hMSH2* (25).

We analyzed a case of PUNLMP and its ANT for MMR mRNA expression. The normal urothelium adjacent to PUNLMP revealed regular or elevated (≥1) mRNA levels of MutSα complex which detects single base-base mismatches and insertion-deletion loops while the mRNA levels of *hMLH1*, a crucial component of MutLα that is responsible for repairing the DNA errors (10,14), were <1. This is in agreement with the results of a previous study which showed that MLH1 is expressed at a lower level than MSH2 and MSH6 in human cells (35), suggesting a regular proliferation of urothelium cells and a limited DNA repair requirement. *hMSH2*, *hMSH6* and *hPMS2* mRNAs were reduced in PUNLMP compared with its ANT, probably due to a low rate of apoptosis (36).

The correlation of our results with clinical data revealed the statistically significant association of *hMSH2* and *hMLH1*, *hMSH2* and *hMSH6*, *hMSH6* and *hPMS2*, *hMLH1* and *hMSH6* tumor/ANT mRNA expression ratios in females. We derive the conclusion that the urothelium of females has a better balance in the expression DNA MMR genes compared with males, who exhibited imbalance. Most likely, the MMR mechanisms are biologically differently regulated in the two genders. Additionally, a significant association was also found between the changes in *hMSH2* and *hMLH1* mRNA expression levels in UCCs compared with their ANTs, indicating that *hMSH2* and *hMLH1* cooperation in DNA repair (10,11,14) requires an associated mechanism for regulating *hMSH2* and *hMLH1* gene expression.

The biological significance of these findings is indicated by the association between *hMSH2*, *hMLH1*, *hMSH6* and *hPMS2* mRNA expression in our tissue cohort. We identified a significant association between reduced mRNA expression levels of *hMSH2*/*control* and *hMSH6*/*control*, indicating a common mechanism of *hMSH2* and *hMSH6* suppression of transcriptional activation that is in accordance with their biological function, as components of the MutSα complex act cooperatively (11-13). The interdependence of the four genetic loci was shown by the observed and calculated frequencies of their combined phenotypes (Table IV) (31). *hMSH2* and *hMSH6* revealed different frequencies and were considered as depended loci, as were *hMSH2* and *hPMS2* or *hMSH6* and *hPMS2* (37). Besides, *hMSH2* and *hMLH1*, *hMHL1* and *hMSH6* or *hMHL1* and *hPMS2* exhibited identical observed

and calculated frequencies in UCCs and/or their ANTs and were considered as independent loci (16).

The identification of MSI in bladder tumors vs. their ANTs and correlation with MMR mRNA expression or MMR phenotypes showed that MSI-H was absent, MSI-L was rare in our study group and LOH was found in a small proportion of informative UCC samples. This result is in agreement with those of previous studies which reported the absence or low frequencies of MSI in bladder cancer (32,38). LOH and MSI-L were observed in a region distal to the *hMLH1* locus. The two UCCs affected by LOH at 3p loci exhibited regular or elevated MMR phenotypes. Therefore, allelic imbalance at these chromosomal regions which harbor *hMLH1* was not correlated with loss of *hMLH1* mRNA expression; this is in agreement with a previous study of non-small cell lung tumors (28). However, the UCCs affected by LOH showed reduced *hMSH6* mRNA tumor/ANT ratios, which may mean that genetic instability in the bladder, distal to the *hMLH1* locus, is correlated with a reduced expression of *hMSH6*.

In conclusion, this is the first study to quantify MMR mRNA expression in bladder tumors and adjacent normal urothelium. Reduced (r) mRNA phenotypes of *hMSH2*, *hMSH6* and *hPMS2* were found to be correlated with precancerous or cancerous urothelium and a previously unrecognized reduced r_2r_6 (*hMSH2* and *hMSH6*) phenotype with a precancerous urothelium. Additionally, we did not identify a reduced r_1 phenotype of *hMLH1*, a crucial component of MutLα complex, in UCCs or their ANTs and *hMLH1* was overexpressed in a significant proportion of UCCs. Therefore, the *hMLH1*-elevated (R_1) mRNA phenotype and mRNA overexpression was correlated with urothelium with malignant potential. The correlation of our results with clinical data revealed that in males the MMR mechanism appears to be unbalanced relative to females and gradually elevated mRNAs expression levels of *hMSH2*, *hMLH1* and *hPMS2* in males show a progression from low to high grade and from pT_a to pT_{1-2} tumors. Biologically, we demonstrated that *hMSH2*, *hMSH6* and *hPMS2* are interdependent loci; particularly, *hMSH2* and *hMSH6* were indicated to have a common mechanism of suppressing transcriptional activation. *hMLH1* was independent, but requires an association with a *hMSH2* mechanism, frequently in low grade tumors, for regulation of mRNA expression. Finally, reduction of *hMSH2* and *hMLH1* mRNA expression in UCCs is unlikely to be correlated with allelic imbalance at polymorphic regions which harbor the genes; however, LOH distal to *hMLH1* may be correlated with *hMSH6* reduction.

References

1. Lee TK, Chaux A, Karram S, Miyamoto H, Miller JS, Fajardo DA, Epstein JI and Netto GJ: Papillary urothelial neoplasm of low malignant potential of the urinary bladder: clinicopathologic and outcome analysis from a single academic center. Hum Pathol 42: 1799-1803, 2011.
2. MacLennan GT, Kirkali Z and Cheng L: Histologic grading of noninvasive papillary urothelial neoplasms. Eur Urol 51: 889-898, 2007.
3. Chaux A, Karram S, Miller JS, Fajardo DA, Lee TK, Miyamoto H and Netto GJ: High-grade papillary urothelial carcinoma of the urinary tract: a clinicopathologic analysis of a post-World Health Organization/International Society of Urological Pathology classification cohort from a single academic center. Hum Pathol 43: 115-120, 2012.
4. Cheng L, Davidson DD, Maclennan GT, Williamson SR, Zhang S, Koch MO, Montironi R and Lopez-Beltran A: The origins of urothelial carcinoma. Expert Rev Anticancer Ther 10: 865-880, 2010.
5. Cordon-Cardo C, Cote RJ and Sauter G: Genetic and molecular markers of urothelial premalignancy and malignancy. Scand J Urol Nephrol (Suppl 205): 82-93, 2000.
6. Cohen SM: Urinary bladder carcinogenesis. Toxicol Pathol 26: 121-127, 1998.
7. Vageli D, Kiaris H, Delakas D, Anezinis P, Cranidis A and Spandidos DA: Transcriptional activation of H-ras, K-ras and N-ras proto-oncogenes in human bladder tumors. Cancer Lett 107: 241-247, 1996.
8. Preston BD, Albertson TM and Herr AJ: DNA replication fidelity and cancer. Semin Cancer Biol 20: 281-293, 2010.
9. Umar A and Kunkel TA: DNA-replication fidelity, mismatch repair and genome instability in cancer cells. Eur J Biochem 238: 297-307, 1996.
10. Marti TM, Kunz C and Fleck O: DNA mismatch repair and mutation avoidance pathways. J Cell Physiol 191: 28-41, 2002.
11. Acharya S, Wilson T, Gradia S, Kane MF, Guerrette S, Marsischky GT, Kolodner R and Fishel R: hMSH2 forms specific mispair-binding complexes with hMSH3 and hMSH6. Proc Natl Acad Sci USA 93: 13629-13634, 1996.
12. Genschel J, Littman SJ, Drummond JT and Modrich P: Isolation of MutSbeta from human cells and comparison of the mismatch repair specificities of MutSbeta and MutSalpha. J Biol Chem 273: 19895-19901, 1998.
13. Umar A, Risinger JI, Glaab WE, Tindall KR, Barrett JC and Kunkel TA: Functional overlap in mismatch repair by human MSH3 and MSH6. Genetics 148: 1637-1646, 1998.
14. Nakagawa T, Datta A and Kolodner RD: Multiple functions of MutS- and MutL-related heterocomplexes. Proc Natl Acad Sci USA 96: 14186-14188, 1999.
15. Ruszkiewicz A, Bennett G, Moore J, Manavis J, Rudzki B, Shen L and Suthers G: Correlation of mismatch repair genes immunohistochemistry and microsatellite instability status in HNPCC-associated tumours. Pathology 34: 541-547, 2002.
16. Vageli D, Daniil Z, Dahabreh J, Karagianni E, Vamvakopoulou DN, Ioannou MG, Scarpinato K, Vamvakopoulos NC, Gourgoulianis KI and Koukoulis GK: Phenotypic mismatch repair hMSH2 and hMLH1 gene expression profiles in primary non-small cell lung carcinomas. Lung Cancer 64: 282-288, 2009.
17. Dietmaier W, Wallinger S, Bocker T, Kullmann F, Fishel R and Rüschoff J: Diagnostic microsatellite instability: definition and correlation with mismatch repair protein expression. Cancer Res 57: 4749-4756, 1997.
18. Mylona E, Zarogiannos A, Nomikos A, Giannopoulou I, Nikolaou I, Zervas A and Nakopoulou L: Prognostic value of microsatellite instability determined by immunohistochemical staining of hMSH2 and hMSH6 in urothelial carcinoma of the bladder. APMIS 116: 59-65, 2008.
19. Yamamoto Y, Matsuyama H, Kawauchi S, Furuya T, Liu XP, Ikemoto K, Oga A, Naito K and Sasaki K: Biological characteristics in bladder cancer depend on the type of genetic instability. Clin Cancer Res 12: 2752-2758, 2006.
20. Catto JW, Xinarianos G, Burton JL, Meuth M and Hamdy FC: Differential expression of hMLH1 and hMSH2 is related to bladder cancer grade, stage and prognosis but not microsatellite instability. Int J Cancer 105: 484-490, 2003.
21. Rubio J, Blanes A, Sanchez-Carrillo JJ and Diaz-Cano SJ: Microsatellite abnormalities and somatic down-regulation of mismatch repair characterize nodular-trabecular muscle-invasive urothelial carcinoma of the bladder. Histopathology 51: 458-467, 2007.
22. Ericson KM, Isinger AP, Isfoss BL and Nilbert MC: Low frequency of defective mismatch repair in a population-based series of upper urothelial carcinoma. BMC Cancer 5: 23, 2005.
23. Saetta AA, Goudopoulou A, Korkolopoulou P, Voutsinas G, Thomas-Tsagli E, Michalopoulos NV and Patsouris E: Mononucleotide markers of microsatellite instability in carcinomas of the urinary bladder. Eur J Surg Oncol 30: 796-803, 2004.
24. Kassem HS, Varley JM, Hamam SM and Margison GP: Immunohistochemical analysis of expression and allelotype of mismatch repair genes (hMLH1 and hMSH2) in bladder cancer. Br J Cancer 84: 321-328, 2001.
25. Thykjaer T, Christensen M, Clark AB, Hansen LR, Kunkel TA and Ørntoft TF: Functional analysis of the mismatch repair system in bladder cancer. Br J Cancer 85: 568-575, 2001.

26. Leach FS, Hsieh JT, Molberg K, Saboorian MH, McConnell JD and Sagalowsky AI: Expression of the human mismatch repair gene hMSH2: a potential marker for urothelial malignancy. Cancer 88: 2333-2341, 2000.
27. Vageli D, Ioannou MG and Koukoulis GK: Transcriptional activation of hTERT in breast carcinomas by the Her2-ER81-related pathway. Oncol Res 17: 413-423, 2009.
28. Wang YC, Lu YP, Tseng RC, Lin RK, Chang JW, Chen JT, Shih CM and Chen CY: Inactivation of hMLH1 and hMSH2 by promoter methylation in primary non-small cell lung tumors and matched sputum samples. J Clin Invest 111: 887-895, 2003.
29. Zhou XP, Hoang JM, Cottu P, Thomas G and Hamelin R: Allelic profiles of mononucleotide repeat microsatellites in control individuals and in colorectal tumors with and without replication errors. Oncogene 15: 1713-1718, 1997.
30. Hoang JM, Cottu PH, Thuille B, Salmon RJ, Thomas G and Hamelin R: BAT-26, an indicator of the replication error phenotype in colorectal cancers and cell lines. Cancer Res 57: 300-303, 1997.
31. Vageli D, Daniil Z, Dahabreh J, Karagianni E, Liloglou T, Koukoulis G and Gourgoulianis K: Microsatellite instability and loss of heterozygosity at the MEN1 locus in lung carcinoid tumors: a novel approach using real-time PCR with melting curve analysis in histopathologic material. Oncol Rep 15: 557-564, 2006.
32. Ericson KM, Isinger AP, Isfoss BL and Nilbert MC: Low frequency of defective mismatch repair in a population-based series of upper urothelial carcinoma. BMC Cancer 5: 23, 2005.
33. Shcherbakova PV, Hall MC, Lewis MS, Bennett SE, Martin KJ, Bushel PR, Afshari CA and Kunkel TA: Inactivation of DNA mismatch repair by increased expression of yeast MLH1. Mol Cell Biol 21: 940-951, 2001.
34. Mao G, Lee S, Ortega J, Gu L and Li GM: Modulation of microRNA processing by mismatch repair protein MutLα. Cell Res 22: 973-985, 2012.
35. Chang DK, Ricciardiello L, Goel A, Chang CL and Boland CR: Steady-state regulation of the human DNA mismatch repair system. J Biol Chem 275: 18424-18431, 2000.
36. Köster F, Schröer A, Fischer D, Greweldinger T, Diedrich K and Friedrich M: Correlation of DNA mismatch repair protein hMSH2 immunohistochemistry with p53 and apoptosis in cervical carcinoma. Anticancer Res 27: 63-68, 2007.
37. Hayes AP, Sevi LA, Feldt MC, Rose MD and Gammie AE: Reciprocal regulation of nuclear import of the yeast MutSalpha DNA mismatch repair proteins Msh2 and Msh6. DNA Repair (Amst) 8: 739-751, 2009.
38. Bonnal C, Ravery V, Toublanc M, Bertrand G, Boccon-Gibod L, Henin D, *et al*: Absence of microsatellite instability in transitional cell carcinoma of the bladder. Urology 55: 287-291, 2000.